Composition and sequence distribution of vinylidene fluoride copolymer and terpolymer fluoroelastomers. Determination by ^{19}F nuclear magnetic resonance spectroscopy and correlation with some properties

Maurizio Pianca, Piergiorgio Bonardelli, Marco Tatò, Gianna Cirillo and Giovanni Moggi

Montefluos CRS, via San Pietro 50, 20021 Bollate, Italy

(Received 11 February 1986; revised 20 June 1986)

^{19}F nuclear matnetic resonance spectra of vinylidene fluoride–hexafluoropropene copolymers and vinylidene fluoride–hexafluoropropene–tetrafluoroethylene terpolymers are reported and discussed. Their interpretation allows average composition and sequence distribution to be determined. Sequence distribution is shown to be relevant in determining the trend of glass transition temperatures and in the study of the mechanism of vulcanization.

(Keywords: vinylidene fluoride copolymers; fluoroelastomers; sequence distribution; fluorine nuclear magnetic resonance spectroscopy; glass transition temperature; vulcanization)

INTRODUCTION

Vinylidene fluoride–hexafluoropropene (VDF–HFP) copolymers and vinylidene fluoride–hexafluoropropene–tetrafluoroethylene (VDF–HFP–TFE) terpolymers are well known fluoroelastomers (tradenames Tecnoflon, Viton, Fluorel, Daiel) suitable for uses at high temperatures or in the presence of aggressive chemicals such as strong acids and bases, high-temperature steam, organic solvents, lubricants etc.[1,2] Their thermal and chemical stability is due to the strong C–F bonds (about 110 kcal mol^{-1} vs. about 100 kcal mol^{-1} for aliphatic C–H bonds) and to the higher strength of C–C bonds in fluorinated compounds (97 kcal mol^{-1} in hexafluoroethane vs. 88 kcal mol^{-1} in ethane).

These polymers are usually prepared by emulsion polymerization[2,3], and therefore the distribution of the different monomer moieties is statistical, though there are no HFP–HFP sequences, as this monomer cannot homopolymerize in the free-radical way[3,4]. The monomer units most often add to the growing radical in such a way that the unpaired electron is localized on the more substituted carbon atom

$$-CH_2-CF_2 \qquad -CF_2-\underset{\displaystyle CF_3}{\overset{\displaystyle |}{CF}}$$

according to the usual 'head-to-tail' reaction pattern. To a lesser extent inversions, i.e. 'head-to-head' and 'tail-to-tail' additions, are also possible.

N.m.r. spectroscopy has been widely used for many years in polymer structure studies, for which completely decoupled ^{13}C spectroscopy is probably the most useful technique. Unfortunately ^{13}C couples with ^{19}F, whose resonance field interval is broader than the band covered by common spin decouplers. Therefore it is troublesome to record decoupled ^{13}C spectra of compounds having a wide ^{19}F spectrum, such as fluoroelastomers. These latter materials can be studied by means of ^{19}F n.m.r., which resonates in an interval broad enough to give adequate structural information.

It is the aim of this work to show that the sequence distribution of co- and terpolymer fluoroelastomers can be deduced from ^{19}F n.m.r. spectra and that it can be related to important properties of the polymers.

EXPERIMENTAL

Synthesis

Co- and terpolymers were prepared by semicontinuous emulsion polymerization in a 5 l stainless-steel stirred autoclave, at 70–100°C and 10–20 atm, with 3.5 l demineralized water, using ammonium persulphate as the free-radical initiator and continuously feeding a gaseous monomer mixture having the same composition as the desired polymer. The initial gas composition in the reactor was adjusted in order to yield the desired polymer composition. The reaction conditions were varied in order to obtain similar Mooney viscosities for all the polymer compositions.

The polymers were coagulated by pouring the latexes into an equal volume of stirred 6 g l^{-1} aluminium sulphate solution, washed with demineralized water and dried at 70°C for 16 h.

0032-3861/87/020224-07$03.00

Table 1 Composition of compounds for vulcanization

Compounds	Weight content (phr)[a]	
	Copolymers	Terpolymers
Elastomer	100	100
Accelerator: $BzP(NMe_2)_3BF_4$	0.375	0.5
Bisphenol AF	1.8	1.5
Magnesium oxide DE	5	5
Calcium hydroxide	5	5
MT carbon black	25	25

[a] phr = parts per hundred parts of rubber

^{19}F *n.m.r. spectra*

The ^{19}F n.m.r. spectra of co- and terpolymers were recorded on a Varian XL-200 spectrometer, at 188.22 MHz, under the following experimental conditions: solvent, acetone-d_6; sample concentration, 10% by weight; observation temperature, 21°C; 240 accumulations; flip angle, 30°; pulse width, 2 μs; pulse delay time, 2 s; spectral window, 30 kHz; memory, 32 K. The main signal of CF_3 groups (78.8 ppm *versus* $CFCl_3$, as determined in a separate experiment) was employed as an internal reference. Upfield chemical shifts (from $CFCl_3$) have been considered as positive.

Glass transition temperatures

Glass transition temperatures (T_g) were measured by differential scanning calorimetry (d.s.c.) using a Perkin–Elmer DSC 2C calorimeter, with a heating rate of 10°C min^{-1}. The intersection of the line of maximum slope with the baseline was adopted as the T_g.

Vulcanization

Rubbers of different composition but having very similar Mooney viscosity were vulcanized in a Monsanto R 100 S rheometer following ASTM 2084, at three different temperatures, with the formulations reported in *Table 1*. Different formulations were adopted for co- and terpolymers because of the slower vulcanization of the latter.

RESULTS AND DISCUSSION

^{19}F *n.m.r. spectra*

VDF–HFP copolymers. The determination of the composition and microstructure of VDF–HFP copolymers was one of the earliest applications of high-resolution n.m.r. methods to polymers[5]. This early work was done at 40 MHz for ^{19}F, and has been followed by other studies, at higher magnetic fields, which showed a better resolution and revealed a wealth of additional details.

Figure 1 shows the spectrum of a VDF–HFP copolymer and *Table 2* reports the assignments of the resonances. The right-hand column of *Table 2* indicates the sequences of monomer units which originate each signal. The symbols used are 0 and 1 for

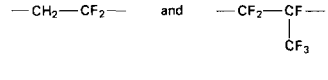

respectively.

The assignments of *Table 2* have been made empirically, as follows: from generalizations concerning the effects of α- and β-carbon atom substituents[5–11]; from variations in the relative intensities of the lines with changes in monomer ratios; and by verification that the relative intensities of the various group resonances are consistent with the assignments.

The following analytical formula can be used to determine the composition of VDF–HFP copolymers:

$$[VDF] = \frac{3\sum CF_2 - 2\sum CF_3}{3\sum CF_2} \quad (1)$$

where [VDF] is the mole fraction of vinylidene fluoride in the polymer, $\sum CF_2$ is the integral of all CF_2 froups (from C to K in *Table 2*) and $\sum CF_3$ is the integral of all CF_3 froups (A + B in *Table 2*).

Monomer inversions ('head-to-head' or 'tail-to-tail' additions) cannot be quantified because inversion either of an HFP unit or of the following VDF unit results in the same structural unit

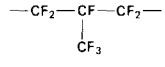

corresponding to signal A in *Table 2*.

First-order Markov statistics are usually necessary to describe the distribution of monomer units in a copolymer, because the probabilities of addition of the two monomers to the growing macromolecule are conditioned by the type of chain-ending radical. As HFP cannot homopolymerize under the reaction conditions employed in the synthesis of VDF–HFP copolymers[3,4], $P_{11} = 0$ and $P_{10} = 1$, whre P_{11} and P_{10} are the probabilities that a growing chain ending in 1 (HFP) adds another 1 (HFP) or a 0 (VDF) monomer unit, respectively. This fact allows the treatment of monomer sequence distribution to be simplified by the introduction of the fictitious monomers

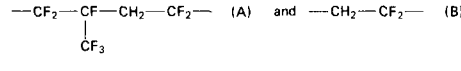

With these 'new' monomers, simpler Bernoullian statistics can be used, in which the probabilities of addition P_A and P_B represent the probabilities of finding the A or B unit in the chain, and correspond to the monomer mole fractions observed in the copolymer:

$$P_A = (10) = N_1/N_0 \quad (2)$$

$$P_B = (0) = (N_0 - N_1)/N_0 \quad (3)$$

where N_0 and N_1 are the mole fractions of VDF and

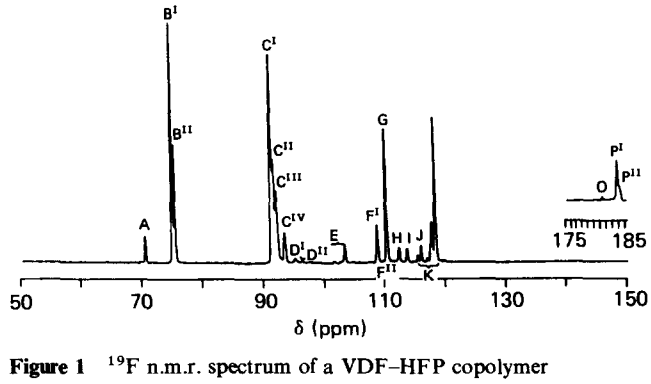

Figure 1 ^{19}F n.m.r. spectrum of a VDF–HFP copolymer

Table 2 Vinylidene fluoride–hexafluoropropene copolymers. Assignments of ^{19}F n.m.r. resonances

Signal	δ (ppm vs. $CFCl_3$)	Assignment	Sequence
A	70.3	$CH_2CF_2\underline{C}F(CF_3)CF_2CH_2CF_2$	010
		$CH_2CF_2CF_2\underline{C}F(CF_3)CF_2CH_2$	010
B^I	74.8	$CH_2CF_2CF_2\underline{C}F(CF_3)CH_2CF_2$	010
		$CF_2CH_2CF_2\underline{C}F(CF_3)CH_2CF_2$	010
B^{II}	75.2	$CH_2CF_2CF_2\underline{C}F(CF_3)CH_2CF_2CF(CF_3)$	0101
C^I	91.3	$CH_2CF_2CH_2C\underline{F}_2CH_2CF_2CH_2$	0000
C^{II}	91.5	$CH_2CF_2CH_2C\underline{F}_2CH_2CF_2CF_2CF(CF_3)$	0001
C^{III}	92.0	$CF_2(CF_3)CH_2C\underline{F}_2CH_2CF_2CH_2$	1000
C^{IV}	93.3	$CF_2(CF_3)CH_2C\underline{F}_2CH_2CF_2CF(CF_3)$	1001
D^I	95.0	$CF_2CH_2CH_2C\underline{F}_2CH_2CF_2CH_2$	0000
		$CF_2CH_2CH_2C\underline{F}_2CH_2CF_2CF_2CH_2$	0000
D^{II}	96.2	$CF_2CH_2CH_2C\underline{F}_2CH_2CF_2CF(CF_3)$	0001
E	101.4	$CF_2CH_2C\underline{F}_2CF(CF_3)CH_2CF_2$	010
		$CF_2CF(CF_3)C\underline{F}_2CH_2CH_2CF_2$	100
		$CF_2(CF_3)CFCH_2C\underline{F}_2CF(CF_3)CF_2$	100
	102.6	$CH_2CF_2CH_2C\underline{F}_2CF(CF_3)CF_2$	101
	103.2	$CH_2CF_2CF(CF_3)C\underline{F}_2CH_2CF_2$	010
		$CF_2(CF_3)CFC\underline{F}_2CF_2CH_2CF_2CF(CF_3)$	101
F^I	108.6	$CF_2(CF_3)CFCH_2C\underline{F}_2CF_2CF(CF_3)$	101
F^{II}	109.6	$CF(CF_3)CF_2CH_2C\underline{F}_2CF_2CF(CF_3)$	101
G	110.0	$CH_2CF_2CH_2C\underline{F}_2CF_2CF(CF_3)$	001

continued

Table 2 *continued*

Signal	δ (ppm vs. $CFCl_3$)	Assignment	Sequence
H	112.1	$CF_2(CF_3)CFCH_2C\underline{F}_2CF_2CH_2$	100
		$CF_2CH_2CH_2C\underline{F}_2CF_2CF(CF_3)$	001
		$CH_2CF_2C\underline{F}_2CH_2CF_2CF(CF_3)$	001
I	113.5	$CH_2CF_2CH_2C\underline{F}_2CF_2CH_2$	000
J	115.9	$CH_2CF_2C\underline{F}_2CH_2CH_2CF_2$	000
K	da 115.3	$CH_2CF_2C\underline{F}_2CF(CF_3)CH_2CF_2$	010
	a 119.5	$CH_2CF_2C\underline{F}_2CF(CF_3)CF_2CH_2$	010
O	182.3	$CH_2CF_2C\underline{F}(CF_3)CF_2CH_2CF_2$	010
		$CH_2CF_2CF_2C\underline{F}(CF_3)CF_2CH_2$	010
P^I	185.0	$CH_2CF_2CF_2C\underline{F}(CF_3)CH_2CF_2CH_2CF_2$	0100
		$CF_2CH_2CF_2C\underline{F}(CF_3)CH_2CF_2$	010
P^{II}	185.2	$CH_2CF_2CF_2C\underline{F}(CF_3)CH_2CF_2CF(CF_3)$	0101

HFP, respectively. For the dyad probabilities:

$$(AA) = P_A^2 = N_1^2/N_0^2 = (101)/N_0 \quad (4)$$

$$(AB) + (BA) = 2P_AP_B = 2N(N_0 - N_1)/N_0^2$$

$$= (100) + (001)/N_0 \quad (5)$$

$$(BB) = P_B^2 = (N_0 - N_1)/N_0^2 = (000)/N_0 \quad (6)$$

On the grounds of the assignments reported in *Table 2*, it is possible to determine experimentally the concentrations of all the possible A–B couples or 1–0 triads, using the following relationships:

$$(BB) = (000) = C^I + C^{II} + C^{III} + C^{IV} - G \quad (7)$$

$$(AB) + BA) = (100) + (001) = 2G \quad (8)$$

$$(AA) = (101) = F \quad (9)$$

where the symbols defined in *Table 2* are the normalized integrals of the corresponding signals.

Figure 2 reports the data of polymers with different monomer ratios, showing the excellent agreement

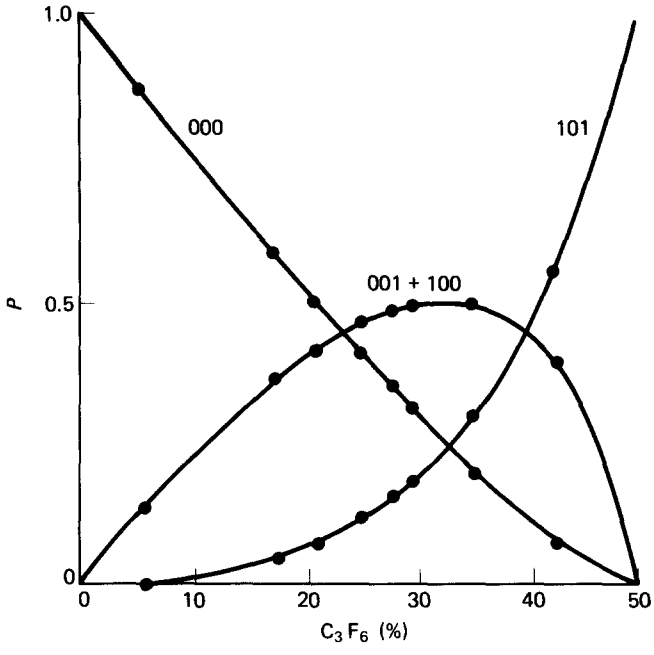

Figure 2 Frequencies of monomer triads as a function of composition of VDF–HFP copolymers: ●, experimental results from ^{19}F n.m.r. spectra; ———, computed values according to the Bernoullian model

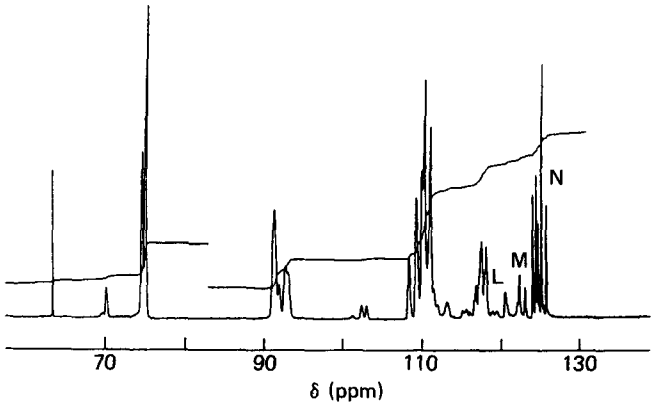

Figure 3 ^{19}F n.m.r. spectrum of a VDF–HFP–TFE terpolymer

between the experimental data and the model proposed. The conformity with the model leads to complete structural resolution of the copolymer and allows, for example, the (number) average sequence lengths $\bar{n}$ to be evaluated, according to the following formulae:

$$\bar{n}_0 = 1/P_{01} \tag{10}$$

$$\bar{n}_1 = 1/P_{10} \tag{11}$$

Hence, for VDF–HFP copolymers:

$$n_0 = N_0/N_1 \qquad n_1 = 1 \tag{12}$$

VDF–HFP–TFE terpolymers. A typical spectrum of a VDF–HFP–TFE terpolymer is shown in *Figure 3*. All signals attributed in *Table 2* (referring to VDF–HFP copolymers) are also present in terpolymer spectra. The presence of TFE units increases the complexity of the signals from F to K and originates the new L, M and N signals of *Figure 3* which will be discussed further in the text.

In approaching the study of terpolymers, we initially attempted to proceed by analogy with copolymers, defining four fictitious monomers (VDF, HFP–VDF, HFP–TFE and TFE) and verifying the effectiveness of Bernoullian statistics. As shown in *Table 3*, this model never agrees with the experimental values for the ratio between signals A (about 70 ppm) and B (about 75 ppm), attributed to the groups

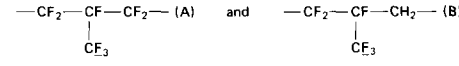

respectively. This ratio is experimentally found to be nearly constant and corresponds to the value observed in VDF–HFP copolymers. Hence we deduce that very little, if any, addition of TFE to HFP occurs. Therefore we can use simpler Bernoullian statistics consisting of three fictitious monomers: VDF (0), HFP–VDF (10) and TFE (2).

The two resonances at about 75 ppm (B) correspond to

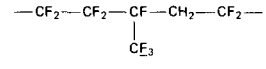

groups. As in copolymers, the CF_3 in the 0100 and 10100 (B^I) sequences are expected to resonate at lower fields with respect to the CF_3 in the sequences:

$$\begin{array}{c} 0\,10\,10 \\ 10\,10\,10 \\ 2\,10\,10 \\ 0\,10\,\;2 \\ 10\,10\,12 \\ 2\,10\,\;2 \end{array} \qquad (B^{II})$$

The computed and experimental probabilities of B^I and B^{II} are compared in *Table 4*. A good accordance is observed.

Table 3 Experimental and calculated values of the ratio between the integrals of the signals at about 70 ppm (A) and 75 ppm (B) in the ^{19}F n.m.r. spectra of VDF–HFP–TFE terpolymers. Calculations according to the Bernoullian model based on four fictitious monomers

		$(A/B) \times 10^2$	
TFE (mol%)	HFP (mol%)	Calc.	Exp.
0	19	0	7.9
0	29	0	7.4
5.1	21	6.9	7.4
9.9	21	14.1	7.3
14.1	21	21.1	7.0
20.3	21	32.5	8.8
23.3	21	38.3	9.3

Table 4 Experimental and calculated relative intensities of the resonances at 74.8 ppm (B^I) and 75.2 ppm (B^{II}) in the ^{19}F n.m.r. spectra of VDF–HFP–TFE terpolymers, Calculations according to the Bernoullian model based on three fictitious monomers

	B^I		B^{II}	
TFE (mol%)	Calc.	Exp.	Calc.	Exp.
5.1	0.62	0.62	0.38	0.38
9.9	0.55	0.56	0.45	0.44
10.2	0.60	0.62	0.40	0.38
14.1	0.60	0.48	0.51	0.52
20.3	0.41	0.41	0.59	0.59
21.7	0.40	0.40	0.60	0.60
23.3	0.39	0.38	0.61	0.62

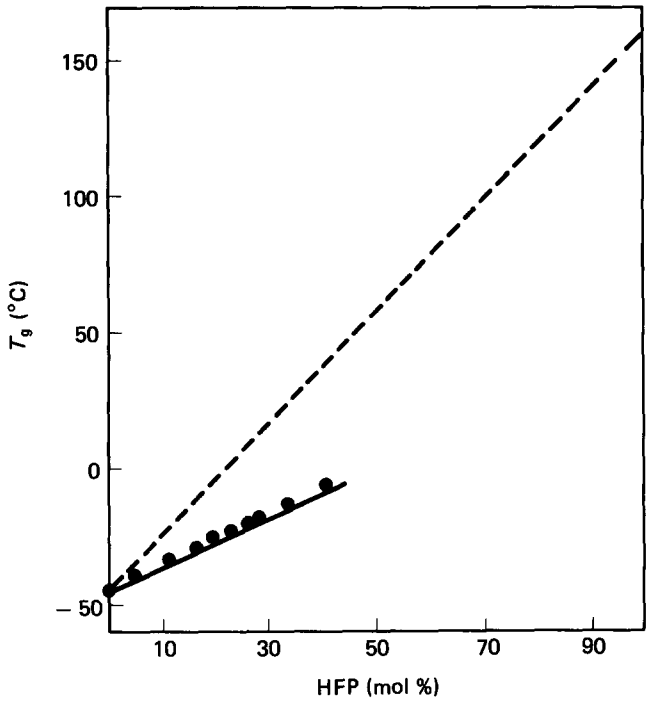

Figure 4 Glass transition temperatures of VDF–HFP copolymers: ●, experimental values; ---, Fox equation; ———, Johnston equation

The signals L, M and N, which do not occur in the spectra of copolymers, are attributed to CF_2 in TFE units, in sequences of decreasing length going towards higher fields. The signal N originates from $-CH_2-CF_2-CF_2-CH_2-CH_2-$, i.e. from a TFE unit between two VDF ones; M is due to $-CH_2-CF_2-CF-CF_2-CF_2-$, and L to $-CF_2-CF_2-CF_2-CF_2-CF_2-$. A more detailed assignment, in terms of monomer sequences, is not possible so far, because of various overlapping signals. Some model compounds necessary for the complete assignments, are in preparation.

The sequential analysis that can be obtained from ^{19}F n.m.r. spectra is very useful in the study of some important properties of co- and terpolymers that depend not only on the average composition but also on the sequence distribution. As examples of such properties we shall discuss below the glass transition temperatures and the vulcanization behaviour.

Glass transition temperatures (T_g)

T_g is a second-order transition of the amorphous phase. It marks the freezing-in (on cooling) or the unfreezing (on heating) of micro-Brownian motion of chain segments 20–50 carbon atoms in length. The micro-Brownian motion is a semi-cooperative action involving torsional oscillations and/or rotations about backbone bonds in a given chain as well as in neighbouring ones. Torsional motion of side groups about the axis connecting them to the main chain may also be involved[12]. All physical and mechanical properties of linear amorphous polymers change in a dramatic fashion at T_g, which marks the border in the broad transition between the rigid solid and the liquid-like region. As a matter of fact the embrittlement below T_g is a practical limit to the low-temperaure applications of elastomers.

Figure 4 shows the T_g of VDF–HFP copolymers[13–15]. The experimental trend is not fitted by the Fox equation[16]

$$\frac{1}{T_g}=\frac{W_A}{T_{g,A}}+\frac{W_B}{T_{g,B}} \tag{13}$$

which does not consider the sequence distribution. In equation (13) W_A and W_B are the weight fractions of the monomers in the copolymer, T_g the glass transition temperature of the copolymer and $T_{g,A}$ and $T_{g,B}$ the T_g of the homopolymers, assumed as $T_{g,VDF}=-45°C$ (our experimental value) and $T_{g,HFP}=160°C$ (average between literature values)[17,18]. In contrast, if the sequence distribution is accounted for, a very good interpolation of the experimental values is obtained by means of the Johnston equation[19,20]:

$$\frac{1}{T_g}=\frac{W_A P_{AA}}{T_{g,A}}+\frac{W_A P_{AB}+W_B P_{BA}}{T_{g,AB}}+\frac{W_B P_{BB}}{T_{g,B}} \tag{14}$$

In equation (14), P_{IJ} are the dyad probabilities and $T_{g,IJ}$ the dyad contributions to T_g. The homopolymer T_g values have been assumed as $T_{g,AA}$ and $T_{g,BB}$, and $T_{gmAB}=0°C$ has been extrapolated from experimental data shown in *Figure 4*.

Extension of equations (13) and (14) to terpolymers is immediate, but some trouble arises in applying the Johnston equation, because of the variety of values reported for the T_g of PTFE. Moreover it has been shown[21] that the T_g of PTFE as extrapolated from copolymers depends on the comonomer. We have chosen $T_{g,PTFE}=11°C$, extrapolated from TFE–(1,1,1-trifluoropropene) copolymers[22]. The T_g contributions of the alternating sequences have been determined according to Couchman[23,24]:

$$T_{g,AB}=(T_{g,A}T_{g,B})^{1/2} \tag{15}$$

The results are shown in *Table 5*. Again, the Fox equation is in complete disagreement with experiment. In contrast, the sequence distribution approach of the Johnston equation yields quite good results.

Vulcanization

Though diamine curing has been widely employed in the past and peroxide curing has been developed for some end uses[1,2], the most common vulcanization system for fluoroelastomers is based on formulations consisting of:

(a) inorganic bases, e.g. $Ca(OH)_2$, MgO;
(b) bisphenol AF,

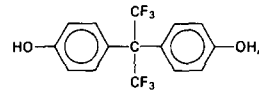

Table 5 Experimental and predicted glass transition temperatures of VDF–HFP–TFE terpolymers

VDF (mol%)	HFP (mol%)	TFE (mol%)	$T_{g,exp}$ (K)	T_g(K) Fox	T_g(K) Johnston
35.6	32.8	31.6	271.5	318.3	269.5
49.4	18.4	32.2	264.5	289.6	266.7
55.4	13.0	31.6	260.5	277.6	264.0
60.3	24.1	15.6	259.5	293.6	261.5
61.2	16.5	22.3	255.4	280.4	257.5
63.8	27.8	8.3	258.0	298.3	260.0
64.3	19.1	16.6	253.5	283.0	258.8
71.8	20.7	7.5	252.0	284.6	257.6

(c) a vulcanizing accelerator, generally a quaternary salt of 'onium' (ammonium, phosphonium, etc.);
(d) fillers, such as carbon black.

According to the currently accepted mechanism, the crosslinking reaction consists of two steps:

(1) polymer dehydrofluorination by the base, to give double bonds in the backbone chain:

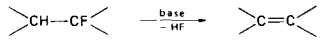

(2) nucleophilic addition of bisphenol AF to the double bonds, yielding crosslinks:

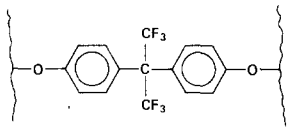

It is worth reminding ourselves that carbon–carbon double bonds in fluorinated compounds are electrophilic.

The accelerator, which has the structure typical of phase transfer catalysts, is thought to act as the cation of the base and/or bisphenate, making them able to diffuse through the rubber.

Schmiegel[24,25] has observed that solution reaction with bases of VDF–HFP copolymers results in the decrease of the integrated intensity of the 75.2 and 108.6 ppm signals in the ^{19}F n.m.r. spectrum, corresponding to

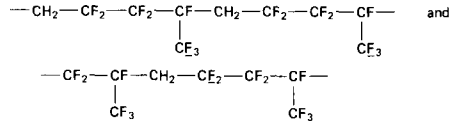

respectively. After the basic treatment he also observed the appearance of two low-field small resonances, which he attributed to

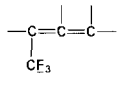

On this basis he suggested that dehydrofluorination takes place selectively on HFP–VDF–HFP sequences to give conjugated dienes, and that the latter are the site of vulcanization:

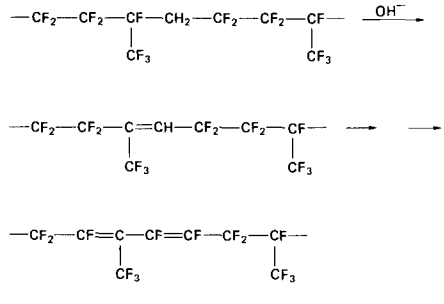

We have tried to get information on the crosslinking mechanism from the vulcanization behaviour[26]. As usual, vulcanization was followed by the torque measured in an oscillating disc rheometer (ODR). As crosslinking proceeds, the rotational viscosity of the sample increases. We focused our attention on two parameters: K, the maximum slope of the torque vs. time curve, is related to the reaction rate; $t_{s,2}$ is the time needed for the torque to rise 2 lb inch above the minimum. Roughly speaking, it may be considered as the time needed to have a double bond concentration high enough to give a detectable vulcanization rate.

If HFP–VDF–HFP sequences were the site of vulcanization, K would be expected to grow and $t_{s,2}$ to shorten on increasing the concentration of such sequences in the polymer. Later on this concentration will be referred to as $F(1)$. The experimental results do not confirm these ideas: increasing $F(1)$ results in a decrease of K and an increase of $t_{s,2}$ (*Figure 5*). As shown in *Figure 6*, K decreases regularly with increasing HFP content. The inversion of the trend at low HFP concentrations might be attributed to chain stiffness: actually the polymer gradually turns from elastomeric to semicrystalline and plastomeric as HFP becomes less than about 17 mol%. *Figure 6* shows also that $t_{s,2}$ becomes longer with growing HFP content.

Similar trends have been observed for VDF–HFP–TFE terpolymers. At a constant molar ratio VDF/HFP of 3:1, increasing the TFE content in the polymer results in reduced K and longer $t_{s,2}$ (*Figure 7*).

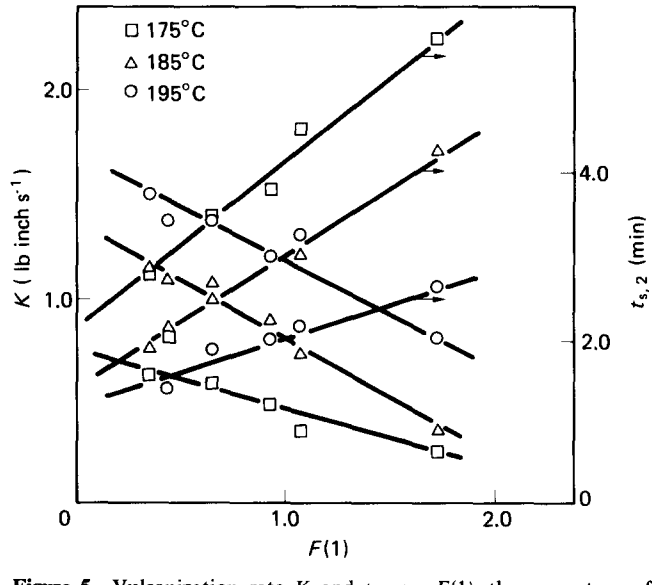

Figure 5 Vulcanization rate K and $t_{s,2}$ vs. $F(1)$, the percentage of HFP–VDF–HFP sequences in VDF–HFP copolymers

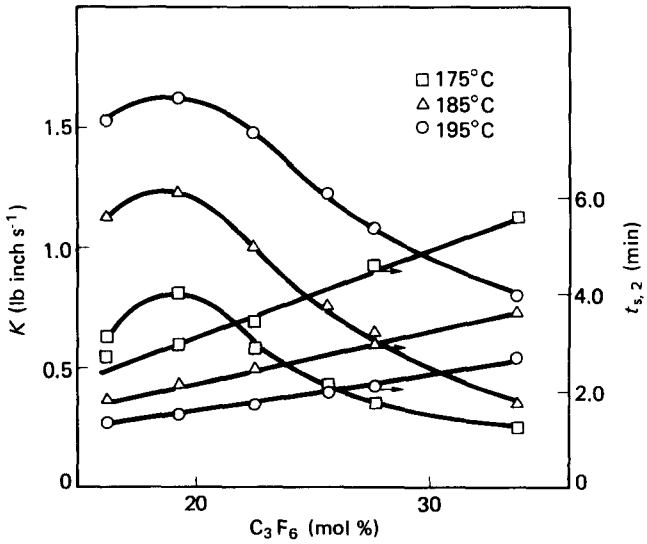

Figure 6 Vulcanization rate K and $t_{s,2}$ of VDF–HFP copolymers

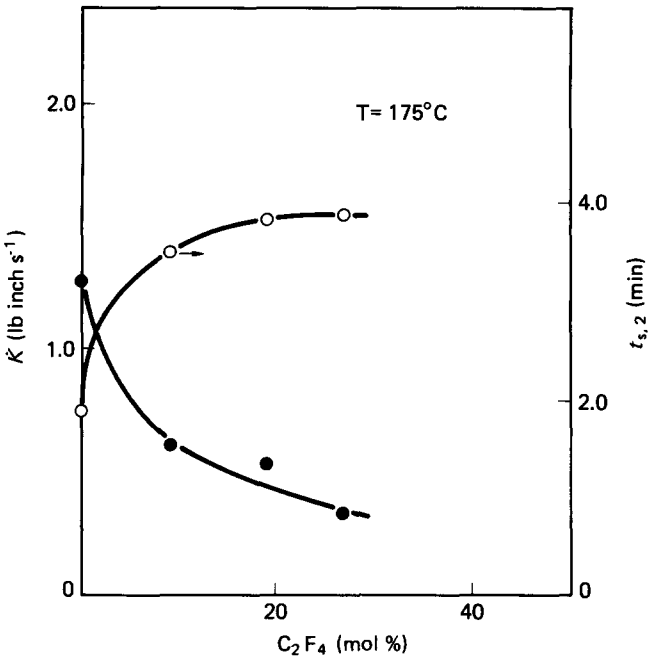

Figure 7 Vulcanization rate K and $t_{s,2}$ of VDF–HFP–TFE terpolymers with a molar ratio VDF/HFP=3

As a whole, the experimental results of ODR measurements do not agree with Schmiegel's mechanism and suggest that the vulcanization behaviour depends more likely on the overall content of VDF, the moiety that can be dehydrofluorinated, than on the presence of HFP–VDF–HFP sequences.

Though Schmiegel's observations make it difficult to think of a fully random dehydrofluorination, at least in solution, the reaction pattern seems to be more complex than that suggested by Schmiegel.

REFERENCES

1 Albin, L. D. *Rubber Chem. Technol.* 1982, **55**, 902 and references therein
2 Arnold, R. G., Barney, A. L. and Thompson, D. C. *Rubber Chem. Technol.* 1973, **46**, 619
3 Dixon, S., Redford, D. R. and Rugg, J. S. *Ind. Eng. Chem.* 1957, **49**, 1687
4 Adam, R. M. and Bovey, F. A. *J. Polym. Sci.* 1952, **9**, 481
5 Ferguson, R. C. *J. Am. Chem. Soc.* 1960, **82**, 2416
6 Ferguson, R. C. *Kautsch. Gummi Kunstst.* 1965, **11**, 723
7 Brame, E. G. and Yeager, F. W. *Anal. Chem.* 1976, **48**, 709
8 Moggi, G., Geri, S., Flabbi, L. and Ajroldi, G. *L'Industria della Gomma* 1980, 268
9 Price, F. P. *J. Chem. Phys.* 1962, **36**, 209
10 Murasheva, Ye. M., Shashkov, A. S. and Galil-Ogly, F. A. *Polym. Sci. USSR* 1979, **21**, 968
11 Murasheva, Ye. M., Shashkov, A. S. and Dontsov, A. A. *Polym. Sci. USSR* 1981, **23**, 711
12 Boyer, R. in 'Encyclopedia of Polymer Science and Technology', Suppl. Vol. 2, Wiley, New York, 1977, p. 745
13 Moggi, G., Bonardelli, P. and Turturro, A. Int. Rubber Conf., Paris, 1982, Preprint I-19
14 Moggi, G., Bonardelli, P., Turturro, A. and Corazza, P. Int. Rubber Conf., Moscow, 1984, Preprint A35
15 Bonardelli, P., Moggi, G. and Turturro, A. *Polymer* 1986, **27**, 905
16 Fox, T. G. *Bull. Am. Phys. Soc.* 1956, **1**, 123
17 Eleuterio, H. S. and Moore, E. P. 2nd Int. Symp. on Fluorine Chemistry, 1962, Estes Park, Col., Preprinte p. 3
18 Brown, D. W. and Wall, L. A. *J. Polym. Sci.* (*A*-2) 1969, **7**, 601
19 Johnston, N. W. *Prepr., ACS Div. Polym. Chem.* 1969, **10**, 609
20 Johnston, N. W. *J. Macromol. Sci., Rev. Macromol. Chem.* 1976, **14B**, 215
21 Brown, D. W. and Wall, L. A. *Polym. Prepr., ACS Div. Polym. Chem.* 1971, **12**, 302
22 Haldon, R. A., Schell, W. J. and Simha, R. *J. Macromol. Sci., Phys. B* 1967, **1**, 759
23 Couchman, P. R. *Nature* 1982, **298**, 729
24 Schmiegel, W. W. *Kautsch. Gummi Kunstst.* 1978, **31**, 137
25 Schmiegel, W. W. *Angew. Makromol. Chem.* 1979, **76–77**, 39
26 Moggi, G., Bonardelli, P. and Cirillo, G. Int. Rubber Conf., Moscow, 1984, Preprint A62